ELSEVIER

Journal of Alloys and Compounds 434–435 (2007) 362–366

Journal of ALLOYS AND COMPOUNDS

www.elsevier.com/locate/jallcom

High-energy ball-milling synthesis and densification of Fe–Co alloy nanopowders by field-activated sintering (FAST)

R. Nicula [a,*], V.D. Cojocaru [a,b], M. Stir [a], J. Hennicke [c], E. Burkel [a]

[a] *Institute of Physics, Rostock University, August-Bebel-Str. 55, D-18055 Rostock, Germany*
[b] *University POLITEHNICA Bucharest, Spl. Independentei 313, RO-77206, Bucharest, Romania*
[c] *FCT Systeme GmbH, Gewerbepark 11, 96528 Rauenstein, Germany*

Available online 28 September 2006

Abstract

Nanocrystalline Fe–Co soft magnetic alloy powders also containing approximately 4% Cr and 1% V were prepared by high-energy mechanical alloying in liquid media (hexane). Bulk nanostructured magnets of 40 mm diameter were obtained by field-assisted sintering (FAST) also known as spark-plasma sintering (SPS). We used a FAST furnace type HPD25-1 (FCT Systeme, Rauenstein, Germany). The FAST method was shown to successfully assist in decoupling densification from microstructural coarsening, mainly due to the limited exposure of the alloy nanopowders to high temperatures during their sintering into nanostructured bulk compacts. Results of chemical and microstructure analysis by SEM/EDX are presented to evidence the achievement of uniform microstructures and absence of composition gradients across sintered bulk specimens in spite of their large size.

Keywords: Nanostructured materials; Powder metallurgy; Mechanical alloying; Sintering

1. Introduction

High-performance magnetic materials operating at high temperatures are essential to applications such as space power generation systems, transformers, magnetomechanical actuators [1]. These important modern applications require novel soft magnetic materials with high remanence and saturation magnetization, low coercivity, low hysteretic and eddy-current losses and high Curie temperatures, together with improved mechanical properties and corrosion resistance. Amorphous or nanocrystalline Fe–Co alloys were recently developed to meet these requirements [1–3]. The potential of nanostructured alloys as modern soft magnetic materials relies on the fact that for grain dimensions D below a critical size the coercivity H_c decreases rapidly ($H_c \propto D^6$) with decreasing grain size, as predicted by Herzer's random anisotropy model [4].

Nowadays, a major technological challenge remains the identification of suitable powder processing routes able to retain both ultrafine microstructures and the exchange coupling between the magnetic nanoparticles within bulk nanostructured magnets operating at elevated temperatures [1]. The need for large magnetic inductions and Curie temperatures imposes strong restrictions on the choice of soft magnetic alloys for high-temperature applications, limited in essence to Fe–Co alloys. For binary Fe–Co alloys, the peak of the Slater–Pauling curve is attained at compositions close to 30% Co [5], while other properties of interest rather favour the equiatomic composition. Nowadays, mechanical properties still limit the wide-scale use of FeCo-based alloys in magnetic components for high-temperature applications [6].

Vanadium and chromium additions are well known to increase the alloy resistivity (leads in turn to the reduction of eddy-current losses) and improve the FeCo-based alloy formability (for e.g. ductility [7]) during thermomechanical processing, while typical energy products remain comparable to ALNICO-type magnets [8].

The high-density of grain boundaries and the large surface areas specific to nanomaterials cause the dominance of surface and grain-boundary diffusion over volume diffusion for crystallite sizes less than 100 nm. Both these interface diffusion mechanisms provide a strong driving force for densification and coarsening of the microstructure. The densification of nanocrystalline materials up to near theoretical density by conventional sintering methods is often accompanied by

* Corresponding author. Tel.: +49 381 498 6869; fax: +49 381 498 6862.
E-mail address: nicula@physik1.uni-rostock.de (R. Nicula).

0925-8388/$ – see front matter © 2006 Elsevier B.V. All rights reserved.
doi:10.1016/j.jallcom.2006.08.150

anomalous grain growth [9], due to prolonged exposure to high temperatures.

Novel sintering approaches that rely on the kinetic suppression of grain growth were lately exploited to decouple specimen densification from coarsening in nanomaterials. Non-isothermal sintering at ultrafast heating rates was shown to avoid coarsening due to surface diffusion at lower temperatures [10]. More recent attempts to synthesize nanostructured solids use the mechanical activation of powder materials by high-energy ball-milling [11–13], followed by pulsed electric current application during their low pressure consolidation by field-activated sintering (FAST) [14–16], which is similar to spark-plasma sintering (SPS) [17]. The aim of the present work is to evaluate the feasibility of FAST/SPS technology as a suitable processing method for the production of bulk nanocrystalline FeCo-based magnets.

2. Experimental

High-purity iron (Riedel-de-Häen, 99.99%), cobalt (Fluka, 99.8%), vanadium (Mateck, 99.5%) and chromium (Alfa Aesar, 99.9%) powders were used for the mechanosynthesis of Fe–Co–V–Cr alloys using a high-energy planetary ball-mill (RETSCH PM400, DLR, Germany). Appropriate amounts of elemental powders were loaded into hardened steel vials together with stainless steel balls (ball-to-powder ratio, BPR ≈ 15:1). The powder precursors were ball-milled for 80 h in hexane at an angular speed of 250 rotations/min.

The thermal phase stability of the Fe–Co–Cr–V alloy powders upon constant-rate heating at 0.33 K/s. was studied using differential scanning calorimetry (NETZSCH DSC Pegasus 404C).

In situ synchrotron radiation powder diffraction experiments were performed at the high-resolution diffractometer [18] of the B2 HASYLAB beamline (DESY Hamburg), using a STOE furnace operating in inert-gas atmosphere and an OBI image-plate detector [19]. The X-ray diffraction (XRD) patterns ($\lambda = 0.05$ nm) were collected in transmission mode during heating up to 900 °C at 3 °C/min.

The consolidation of the Fe–Co–Cr–V nanopowders into disk-shaped pellets (40 mm diameter, 3 mm thickness, Fig. 1) was conducted by field-assisted sintering FAST using a direct heating hydraulic press (FCT HPD25-1, FCT Systeme, Germany). Sintering by FAST was performed in vacuum, under an uniaxial pressure of 125 MPa. We used a pulsed DC voltage (5 pulses ON/1 pulse OFF, pulse duration 10 ms). The temperature was at first raised to 650 °C at a fast heating rate of 200 °C/min, followed by a short dwell-time of only 60 s at this sintering temperature. The microstructure and chemical composition analysis was performed on both as-milled powders and on FAST sintered compacts using a DSM 960A (ZEISS) electron microscope.

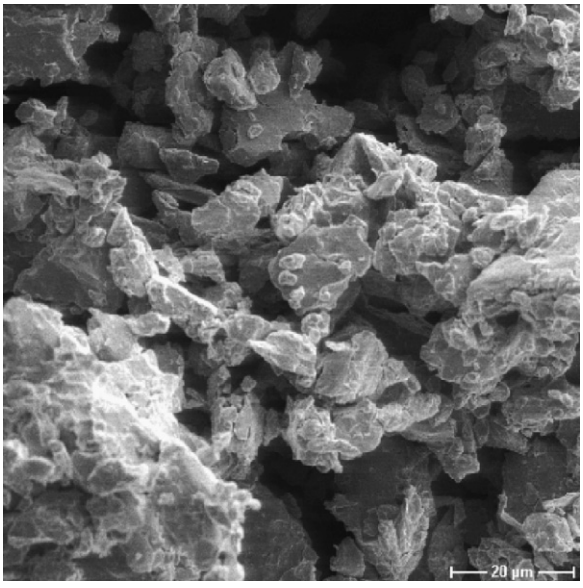

Fig. 1. Typical morphology of the as-milled Fe–Co–Cr–V nanopowders.

3. Results

During high-energy ball-milling, the initial shape of the starting powder particles is lost and the powder particles are flattened by severe plastic deformation processing. Subsequent cold welding leads to the formation of solid-solution/alloy phases as lamellar aggregates. These aggregates will further undergo fragmenting once the cold working limit is reached. The competing cold welding and fragmentation balance towards an equilibrium morphology for long ball-milling times. Beyond a certain milling time no further refinement of the microstructure occurs and the equilibrium morphology is usually given by a bimodal particle-size distribution [20]. The typical alloy morphology after 80 h wet-milling (Fig. 1) is given by particles (2–10 μm) cold welded onto larger aggregates (20–40 μm). A few powder particles still exhibit layered-type structures typical for the ball-milling processing of ductile–ductile powders.

The average chemical composition of the as-milled Fe–Co–Cr–V alloy nanopowders was investigated by energy-dispersive X-ray microanalysis (EDX): the as-milled powders contain 59.84 ± 0.55 wt.% Fe, 35.08 ± 0.53 wt.% Co, 1.21 ± 0.1 wt.% V and 3.87 ± 0.16 wt.% Cr, respectively (Fig. 2).

The DSC trace obtained upon cooling at 40 °C/min (Fig. 3) exhibits an exothermal event at 680 °C corresponding to the α′–α order–disorder transition. The exothermal peak at 960 °C is due to the reversible α(BCC)–γ(FCC) transition.

The *in situ* high-temperature synchrotron radiation diffraction patterns are shown in Fig. 4. The as-milled nanopowders consist of an α-Fe(Co) solid solution with body-centred cubic (BCC) structure. The α′–α order–disorder transition at temperatures above 600 °C cannot be observed, due to the very low intensity of the superlattice reflections of the ordered α′ phase (CsCl-type) [21].

The instrumental resolution function $\beta_0(2\theta)$ was determined using a LaB_6 standard (NIST 660a) and modelled by the Caglioti

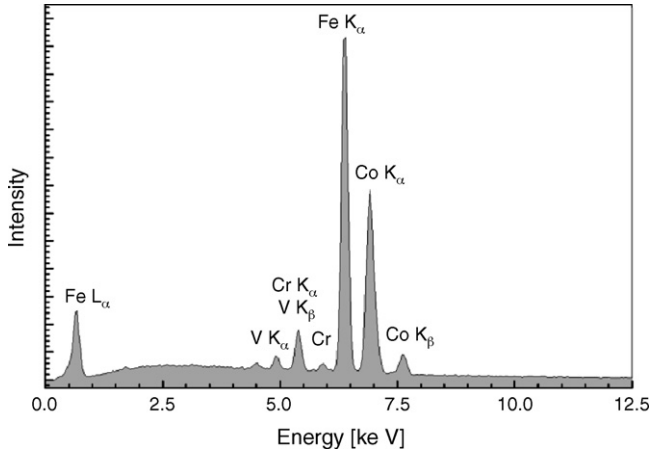

Fig. 2. Typical EDX spectra of the as-milled Fe–Co–V–Cr powders.

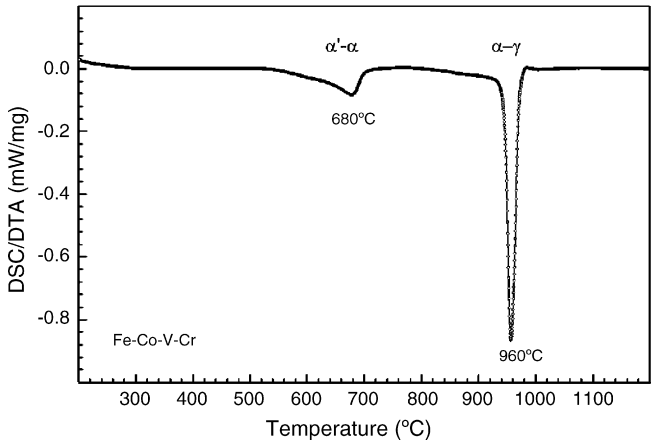

Fig. 3. DSC trace of Fe–Co–Cr–V alloy.

relation:

$$\beta_0 = \sqrt{U\tan^2\theta + V\tan\theta + W} \quad (1)$$

with β_0 the full-width-at-half-maximum (FWHM) of the LaB_6 NIST standard. The Caglioti parameters $U = 0.00309$, $V = 0.0006$ and $W = 0.00151$ were obtained by least-square fitting. The instrumental broadening correction on the specimen FWHM β was then performed according to:

$$\beta_c^2 = (\beta - \beta_0)\sqrt{\beta^2 - \beta_0^2} \quad (2)$$

known as the parabolic Halder–Wagner correction [22]. The corrected linewidths of the (1 1 0) Bragg reflection at different temperatures were used to estimate the temperature evolution of the average crystallite size using the Scherrer equation (Fig. 5).

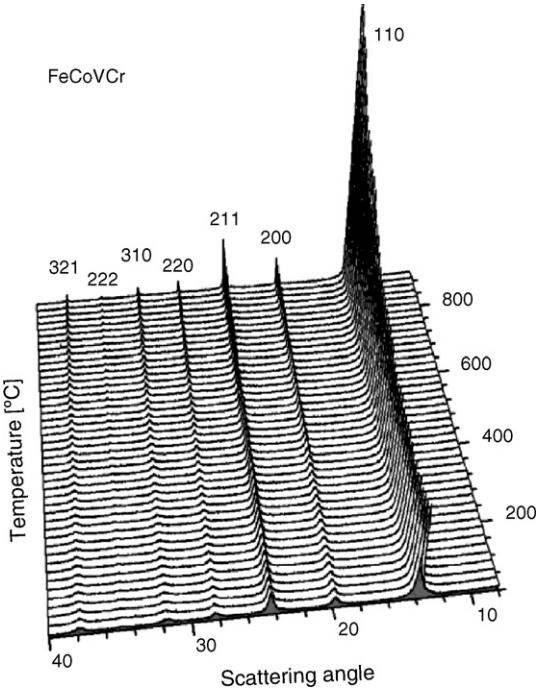

Fig. 4. Synchrotron radiation diffraction patterns obtained during constant-rate heating up to 900 °C.

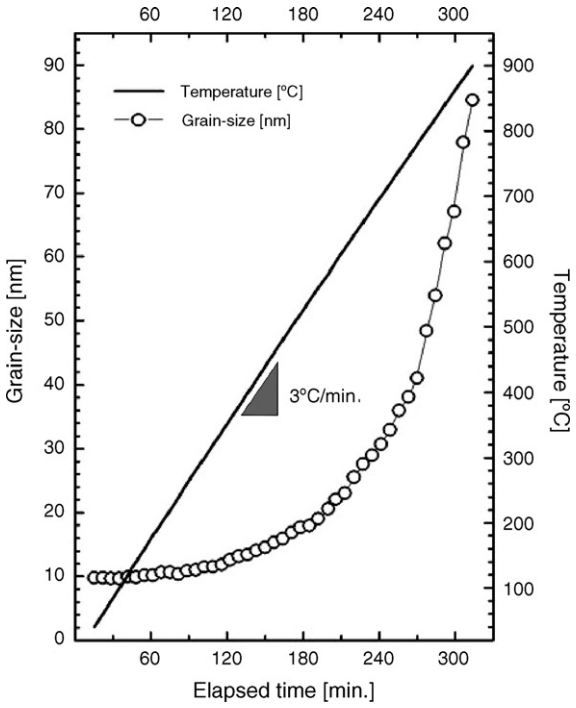

Fig. 5. Grain-size evolution during constant-rate heating of the Fe–Co–Cr–V nanopowders.

The average grain size is found to increase from 10 to 85 nm upon continuous heating at 3 °C/min up to 900 °C.

The linear coefficient of thermal expansion (CTE) was also obtained from the temperature evolution of the unit-cell volume, as modelled by a parabolic function of temperature between 24 and 900 °C. The CTE of the Fe–Co–Cr–V powders equals 16.43 ppm/°C, which is comparable with that of pure iron.

The typical morphology of the FAST/SPS sintered compacts (fracture surface) is illustrated in Fig. 6. The microstructural features of the starting (as-milled) powders are not altered during

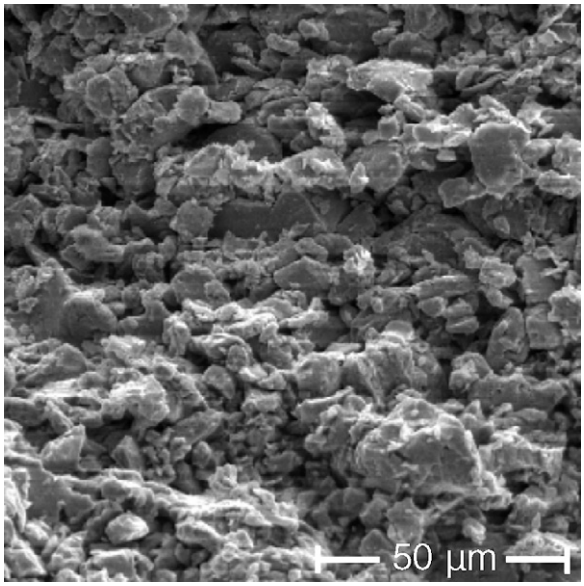

Fig. 6. Fracture surface morphology of Fe–Co–Cr–V pellets FAST sintered for 1 min at 650 °C.

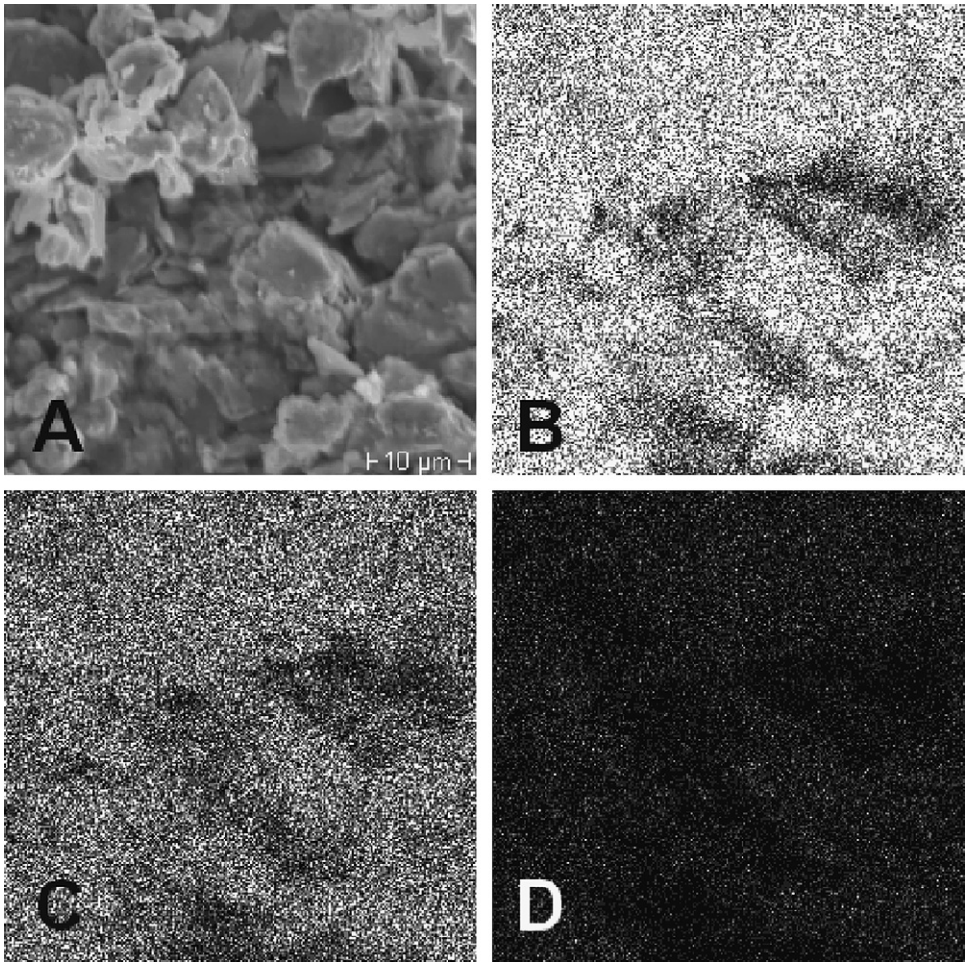

Fig. 7. EDX composition maps of the region (A) (bright image), showing the spatial distribution of Fe (B), Co (C) and Cr (D).

sintering by FAST: most powder particles have sizes between 10 and 20 μm; larger aggregates of up to about 40 μm are also observed. During sintering, the powder particles are welded together and most of the large size pores are removed. The relative density of the FAST sintered parts is close to 95% theoretical density (Archimedes method).

The chemical homogeneity of the sintered parts was also evaluated using composition mapping by SEM/EDX (Fig. 7). Chemical composition analysis performed over an area of 40 μm × 40 μm reveals that Fe, Co and Cr constituents are uniformly distributed within the sintered material.

We may conclude that fast heating combined with short holding times at the sintering temperature successfully yields high-density sintered compacts. The sintered magnets have highly homogeneous microstructures and exhibit an uniform composition throughout their volume.

4. Conclusions

Fe–Co–Cr–V nanopowders with an average grain size of 10 nm were prepared by high-energy ball-milling. Constant-rate heating at 3 °C/min results in an increase of the average grain size to 85 nm at 900 °C. Bulk nanostructured Fe–Co–Cr–V magnets (40 mm diameter) were obtained by FAST/SPS processing within very short times (a few minutes, typically). The FAST/SPS technology preserves the initial fine microstructure of the as-milled powders. Electron microscopy analysis by SEM/EDX could clearly evidence the absence of significant thermal field or chemical composition gradients throughout the entire volume of the sintered parts. The electric field/pulsed current application favours the strong interparticle bonding and the rapid densification of the nanocrystalline powders, without coarsening of the microstructure. Excessive grain growth may still occur at sintering temperatures higher than 900 °C [23,24]. FAST/SPS processing at lower sintering temperatures under high applied pressure could provide an efficient way to avoid unwanted abnormal grain growth effects and to attain higher densities of the sintered compacts.

Acknowledgements

We acknowledge the friendly support of C. Bähtz and M. Knapp (TU-Darmstadt) at the B2 beamline in HASYLAB/DESY (Hamburg). We thank Prof. L. Jonas and G. Fulda (EMZ Rostock) for their kind assistance. This work was performed in the frame of the European Marie Curie Host Programme (HPMD-CT-2001-00089) and was supported by a DAAD-NSF collaborative grant.

References

[1] M.E. McHenry, M.A. Willard, D.E. Laughlin, Prog. Mater. Sci. 44 (1999) 291–433.

[2] M.A. Willard, D.E. Laughlin, M.E. McHenry, J. Appl. Phys. 87 (2000) 7091.

[3] M.E. McHenry, D.E. Laughlin, Acta Mater. 48 (2000) 223–238.

[4] G. Herzer, in: B. Idzikowski, P. Svec, M. Miglierini (Eds.), Properties and Applications of Nanocrystalline Alloys from Amorphous Precursors, Kluwer Academic Publishers, 2005, pp. 15–34 and references therein.

[5] J.M. McLaren, T.C. Schulthess, W.H. Butler, R. Sutton, M. McHenry, J. Appl. Phys. 85 (8) (1999) 4833–4835.

[6] A. Duckham, D.Z. Zhang, D. Liang, V. Luzin, R.C. Cammarata, R.L. Leheny, C.L. Chien, T.P. Weihs, Acta Mater. 51 (2003) 4083–4093.

[7] J.H. White, C.V. Wahl, U.S. Patent 1 862 559 (1932).

[8] H. Matsumoto, N. Ikuta, T. Fujiwara, K. Konno, T. Nomoto, M. Matsuura, H. Taketomi, H. Yoshikawa, S. Takahashi, H. Kaga, J. Magn. Magn. Mater. 272–276 (2004) e1873–e18765.

[9] S. Seal, S.C. Kuiry, P. Georgieva, A. Agarwal, Mater. Res. Soc. Bull. (2004) 16–21.

[10] V.V. Skorokhod, A.V. Ragulya, in: G.-M. Chow, N.I. Noskova (Eds.), Features of Nanocrystalline Structure Formation on Sintering of Ultrafine Powders, Kluwer Academic Publishers, 1998, pp. 387–404.

[11] Z.A. Munir, F. Charlot, F. Bernard, E. Gaffet, US Patent Application 09/374,049 (1999).

[12] Z.A. Munir, J. Mater. Synth. Process. 8 (2000) 189–196.

[13] S. Paris, E. Gaffet, F. Bernard, Z.A. Munir, Scripta Mater. 50 (2004) 691.

[14] J.R. Groza, ASM Handbook, vol. 7: Powder Metallurgy, ASM International, Materials Park, OH, 1998, pp. 583–589.

[15] J.R. Groza, in: C. Suryanarayana (Ed.), Non-equilibrium Processing of Materials, Pergamon, Oxford, UK, 1999, p. 347.

[16] J.R. Groza, A. Zavaliangos, Rev. Adv. Mater. Sci. 5 (2003) 24–33.

[17] M. Tokita, Mater. Sci. Forum 308–311 (1999) 83.

[18] M. Knapp, C. Bähtz, H. Ehrenberg, H. Fuess, J. Synchrotron Radiat. 11 (2004) 328–334.

[19] M. Knapp, V. Joco, C. Bähtz, H.H. Brecht, A. Berghäuser, H. Ehrenberg, H. von Seggern, H. Fuess, Nucl. Instrum. Meth. A 521 (2004) 565–570.

[20] C. Suryanarayana, Prog. Mater. Sci. (2001) 1–184.

[21] J. He, F. Zhou, G. Chang, E.J. Lavernia, J. Mater. Sci. 36 (2001) 2955–2964.

[22] N.C. Halder, C.N.J. Wagner, Acta Cryst. 20 (1966) 312.

[23] Y.D. Kim, J.Y. Chung, J. Kim, H. Jeon, Mater. Sci. Eng. A 291 (2000) 17–21.

[24] B.-H. Lee, S.S. Hong, K.H. Lee, Y.D. Kim, J. Alloys Compd. 385 (2004) 264–268.